A. E. Ruehli

Inductance Calculations in a Complex Integrated Circuit Environment

Abstract: This paper describes a method for calculating multiloop inductances formed by complicated interconnection conductors. Knowledge of these inductances leads to useful information concerning the design of such systems. In the approach pursued here, the conductor loops are divided into segments for which so-called partial inductances are calculated. The partial inductances are then appropriately added to yield the desired loop inductance.

1. Introduction

Historically, inductance calculations have been used primarily in power engineering applications. While little attention is given in most field theory texts to inductance calculations for electronic circuit geometries of practical importance, Grover [1] provides a more extensive treatment of this subject. Additionally, Grover supplies a thorough list of references.

In the last decade, integrated circuit technology has opened new areas of application for inductance calculations. Previously, the role of inductance in electronic circuits and digital systems was mostly limited to discrete components. The coupling among these components could be ignored. In the microcircuit environment, however, complicated multiconductor structures serve as interconnections. The electrical characterization of such structures is doubly important since coupled voltages, signal delays and signal distortion all degrade system performance. Analysis of the electrical properties of multiconductor systems is also fundamental to system synthesis and optimization.

The present paper is devoted to the evaluation of inductances for arbitrary microcircuit geometries. This usually constitutes a first step in the analysis of interconnection systems.

A new comprehensive theory of inductance is offered, which is called the theory of partial inductance since the calculations are based on the inductance of loop segments. This formulation establishes a relationship between incomplete loops and closed loops and thus accommodates Weber's caveat: "It is important to observe that inductance of a piece of wire not forming a closed loop has no meaning" [2]. Further, the theory presented here is fundamental to a complete analysis via partial-element equivalent circuits [3]. All important aspects of modern inductance calculations in integrated circuit systems are discussed. Special attention is given to systems without a local ground plane since the usual two-dimensional calculations become invalid for this case. New formulations are given that are suitable for implementation on a digital computer. (As a practical consideration, computer analysis is the only way to qualitatively characterize these minute structures because of their complexity.) The size of the structures to be considered is small compared to the wavelength of the highest frequency involved, and the overall dimensions are typically less than three centimeters. The conductors, for example, can be lines on a planar surface or small conductor pins. This makes a quasi-static analysis feasible up to relatively high frequencies, as will be shown in Section 3.

The conductors to be analyzed can include both connections within the integrated circuits on the chip and interconnections to the chip. The "on-chip" inductances are generally so negligible that their reactances can be ignored. (This assumption can be substantiated in each particular case by the techniques developed here.) As a further application for this work, the analysis and design of lumped-element microwave circuits is mentioned, e.g. [4]. The approach pursued here is related to a computer

approach for the calculation of magnetic fields [5] in that segmenting of the currents is used in both cases.

Inductances in a multiloop environment are the subject of the next section in this report, while the frequency, where current spreading (nonuniform current distribution) becomes important, is assessed in Section 3. Concepts and definitions of partial inductances are considered in Section 4, while Sections 5 and 6 are devoted to the actual evaluation of partial inductances. Sections 7 and 8 discuss the application of the theory of partial inductances to complicated two- and three-dimensional structures.

2. Inductances of complex geometries

In this section, inductances are considered for a general N-loop system, shown in Fig. 1(a), which is representative of the conductor arrangements of interest. It is rather theoretical, however, and serves primarily in the development of the method and not as a sample application. To start with, all loops are assumed to be completely closed except for an infinitesimal gap between the connection terminals. The inductances of interest here are those formed by the connections, unlike the usual case in which inductances consist of lumped elements and connections are not significant. The inductances for such an N-loop system are given by the definition below.

• *Definition of inductance*

A set of N^2 inductances is defined for a system of N loops as

$$L_{ij} \equiv \frac{\psi_{ij}}{I_j} \text{ for } I_k = 0 \text{ if } k \neq j\,, \tag{1}$$

where ψ_{ij} represents the magnetic flux in loop i due to a current I_j in loop j.

The inductance can be related to the geometry by the magnetic vector potential $\mathbf{A}$ defined by $\mathbf{B} = \nabla \times \mathbf{A}$. The vector potential generated by a current I_j in loop j is

$$\mathbf{A}_{ij} = \frac{\mu}{4\pi} \frac{I_j}{a_j} \oint_j \int_{a_j} \frac{d\mathbf{l}_j\, da_j}{r_{ij}}\,, \tag{2}$$

where $r_{ij} = |\mathbf{r}_i - \mathbf{r}_j|$ and $d\mathbf{l}_j$ is an element of conductor j with the direction along the axis of the conductor. The area a_j is the conductor cross section perpendicular to the current flow. A uniform current density is assumed to exist in conductor j which is of a constant cross section a_j along the loop. The average magnetic flux ψ_{ij} in loop i is easily related to the vector potential $\mathbf{A}_{ij}$ as

$$\psi_{ij} = \frac{1}{\mathrm{a}_i} \oint_i \int_{a_i} \mathbf{A}_{ij} \cdot \mathrm{d}\mathbf{l}_i \mathrm{d}a_i\,, \tag{3}$$

where a_i represents the constant cross sectional area of conductor i. The inductance for the loops i and j can be found by inserting Eqs. (2) and (3) into Eq. (1):

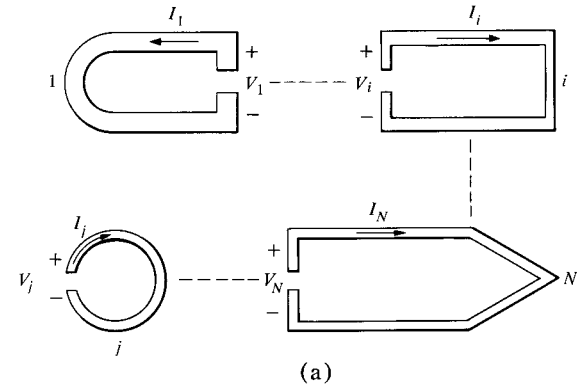

(a)

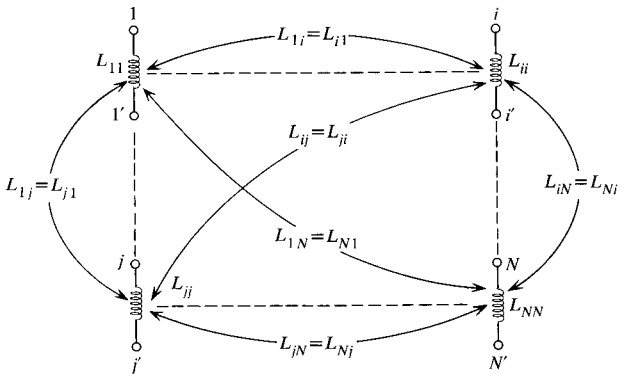

(b)

Figure 1 (a) System of coupled conductor loops. (b) Equivalent circuit for the above geometry.

$$L_{ij} = \frac{1}{a_i a_j} \frac{\mu}{4\pi} \oint_i \int_{a_i} \oint_j \int_{a_j} \frac{d\mathbf{l}_i \cdot d\mathbf{l}_j}{r_{ij}}\, da_i da_j\,. \tag{4}$$

This result can also be derived from energy concepts, but this formulation shows that averages are taken over the conductor cross sections for both the vector potential, Eq. (2), and the flux, Eq. (3). The Neumann formula, which is a special case for the inductance of thin filamentary circuits i and j, is given by

$$L_{\mathrm{f}_{ij}} \equiv \frac{\mu}{4\pi} \oint_i \oint_j \frac{d\mathbf{l}_i \cdot d\mathbf{l}_j}{r_{ij}}\,. \tag{5}$$

The letter f indicates that current filaments are considered. Equation (4) can be written in a simple form with Eq. (5) as

$$L_{ij} = \frac{1}{a_i a_j} \int_{a_i} \int_{a_j} L_{\mathrm{f}ij}\, da_i da_j\,. \tag{6}$$

The idea of the averages is apparent in Eq. (6). For most geometries, closed form solutions for the multiple integrals are hard to find or are unduly complicated. However, the approximation methods presented below result

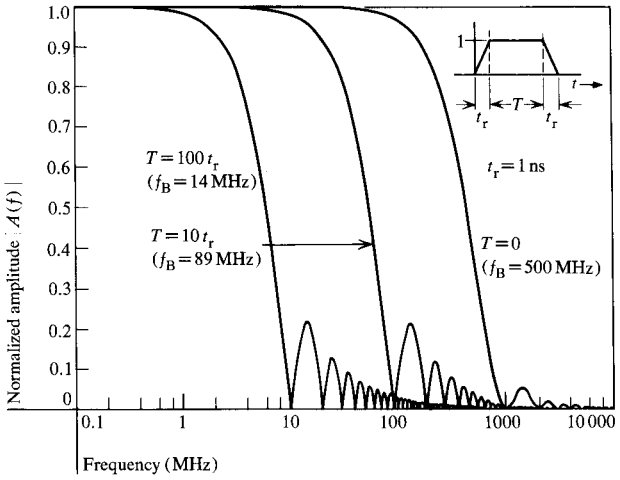

Figure 2 Pulse spectra for different pulse durations T.

in efficient calculations. An equivalent circuit for the configuration of Fig. 1(a) is shown in Fig. 1(b). An $N \times N$ inductance matrix is formed for the system as $\mathbf{L} \equiv [L_{ij}]$ where the elements are, at least in principle, evaluated from Eq. (6). The off-diagonal terms of the L matrix are called mutual inductances, while the diagonal terms are called self inductances. The flux-current relation for the general system of Fig. 1 is

$$\boldsymbol{\psi} = \mathbf{LI}\,. \tag{7}$$

The element ψ_i of the flux vector $\boldsymbol{\psi}$ represents the total flux through the ith loop generated by all N currents. In relation to network analysis, it is desirable to obtain voltage-current relations. Since the voltage is related to the flux by $v_i = \dot{\psi}_i$ it is found in the s-domain that

$$\mathbf{V}(s) = s\mathbf{LI}(s)\,. \tag{8}$$

It is assumed here that the current in all conductors (wires) is uniform or, equivalently, that current crowding effects are small. The next section describes a method for determining the frequency at which current crowding sets in.

3. Estimation of frequency dependence

At first, it seems that Eq. (6) is limited in usefulness by the current redistribution due to eddy currents at high frequencies. However, as shown by the example in Section 7, the change in inductance values is small except in extreme situations where the conductors are placed in close proximity. Further, the length of a bend in a wire conductor is usually small compared with the conductor length. Thus, the current distribution and redistribution with frequency in the corner regions is insignificant for practical calculations and convenient approximations can be applied.

For usual geometries, it is impossible to obtain an accurate estimate of the frequency at which current crowding due to eddy currents becomes important. However, approximate answers can be found from the usual skin-effect calculations [6]. Moderate crowding is expected in conductors with the larger cross section dimension d equal to the skin depth $\delta = (1/\pi f_B \mu\sigma)^{\frac{1}{2}}$, where σ is the conductivity of the conductors. As an example, if the largest cross section d in a system is 0.2mm, then the corresponding frequency f_B is about 0.1 MHz for copper conductors.

Next, a relation is established between the frequency and time domain representations for digital system applications. The amplitude spectrum of the trapezoidal pulse shown in Fig. 2 is found from the Fourier integral to be

$$|A(f)| = (T + t_r)\,|\mathrm{sinc}(ft_r)\mathrm{sinc}\,f(T + t_r)|\,, \tag{9}$$

where T is the pulse duration and t_r the rise time, and $\mathrm{sinc}x \equiv \sin(\pi x)/(\pi x)$. The plot of the normalized amplitude spectrum $|A(f)|$ in Fig. 2 covers a large range of pulse durations T. The pulse duration is variable in a digital system. The curves are easily applied to values of t_r other than 1 ns. If the new rise time is x ns then the new spectrum is found by dividing the frequency scale by x. The frequency f_B to be used in the estimation of the skin distance is found by computation of an equivalent bandwidth

$$f_B = \int_0^\infty |\mathrm{sinc}(ft_r)\mathrm{sinc}\,f(T + t_r)|\,df. \tag{10}$$

The equivalent bandwidth calculations indicated in Fig. 2 are obtained from Eq. (10). The same scaling procedures also apply to the bandwidth calculations. The frequency f_B is then 8.9 MHz for a pulse of 100-ns duration with a 10-ns rise time. The skin depth is, in this case, of the order of 20 μm for copper, a distance smaller than the cross section for most systems.

However, for a conductor spaced at a distance larger than both thickness and width, the inductance will be only a weak function of frequency. This is substantiated by considering Eq. (6), where $L_{f_{ij}}$ is weighted by the nonuniform current distribution. But for conductors spaced sufficiently apart, $L_{f_{ij}}$ is nearly constant over the cross section and thus L_{ij} will be insensitive to the current redistribution. The inductance matrices given in Section 7 serve as examples for the variation of inductance with respect to frequency and conductor spacing.

4. Concepts of partial inductance

This section describes a theory of partial inductance that related to modern network analysis and is suited for computer implementation. This represents a further development of the concepts presented in [1].

The definition of inductance for a particular set of loops is given by Eq. (1). The flux ψ_{ij} is induced in a closed loop where the area is bounded by the loop. It seems, therefore, that no unique flux is associated with an open loop or a segment of wire. It is also obvious that loop j cannot support a current unless the loop is closed in some way. Nevertheless, unique inductances are obtained for incomplete loops as is shown below. Relations for the inductance between parts of circuits can be developed, starting with Eq. (4). For this purpose, the integrations over the lengths are rewritten as summations over the straight loop segments (which may be infinite in number for curved conductors) and all segments are allowed to have a different cross section, or

$$L_{ij} = \sum_{k=1}^{K} \sum_{m=1}^{M} \frac{\mu}{4\pi} \frac{1}{a_k a_m} \int_{a_k} \int_{a_m} \int_{b_k}^{c_k} \int_{b_m}^{c_m} \frac{d\mathbf{l}_k \cdot d\mathbf{l}_m}{r_{km}} da_k da_m . \tag{11}$$

Here, the ith loop is assumed to consist of K segments while the jth loop is divided into M segments. The limits in the integrals are the starting points b_k, b_m and the end points c_k and c_m of the segments.

• *Definition of partial inductance*

Partial inductances are defined in general as the argument of the double summation in Eq. (11) for the conductor segments as

$$L_{\mathrm{p}_{km}} \equiv \frac{\mu}{4\pi} \frac{1}{a_k a_m} \int_{a_k} \int_{a_m} \int_{b_k}^{c_k} \int_{b_m}^{c_m} \frac{|d\mathbf{l}_k \cdot d\mathbf{l}_m|}{r_{km}} da_k da_m . \tag{12}$$

Partial inductances are named $L_{\mathrm{p}_{ij}}$ in order to distinguish them from the loop inductances L_{ij}. (Balabanian and Bickart [7] define the inductance submatrix of the branch impedance matrix as $\mathrm{L_p}$ matrix.)

Sign rule for partial inductances

The sign of $L_{\mathrm{p}_{km}}$ is accounted for by a factor S_{km} given in Eq. (13) below. The choice of the segments into which a circuit is divided is not unique. The lines dividing the conductor loops into parts (for which the partial inductances are to be calculated) are called inductive partitions. There usually exists a set of partitions that is optimal for analysis in each particular case. Then, Eq. (11) is written in general as

$$L_{ij} = \sum_{k=1}^{K} \sum_{m=1}^{M} S_{km} L_{\mathrm{p}_{km}} . \tag{13}$$

S_{km} represents the sign (± 1) associated with the particular partial inductance. The partial inductances $L_{\mathrm{p}_{km}}$ are positive semidefinite by definition. The sign S_{km} has been removed from the purely geometry-dependent partial inductances, since S_{km} depends on the direction of current flow in the conductors.

The evaluation of the sign S_{km} is discussed next. The case of a multiloop situation must be considered for generality. An a priori assignment of terminal voltages and current directions is convenient for generalized calculations. The terminal voltages are always assigned in such a way that the current flows from the positive terminal to the negative terminal. A current vector is assigned to all branches of the loop in the direction of current flow. Then, the sign S_{ij} of the partial inductance $L_{\mathrm{p}_{ij}}$ is determined by the sign of the scalar product between the current vectors i and j. $L_{\mathrm{p}_{ij}}$ is zero for the special case when the scalar product is identically zero for orthogonal currents. If the flux due to the currents assigned to any pair of loops is in the same direction (additive fields), then the coupled voltage is positive.

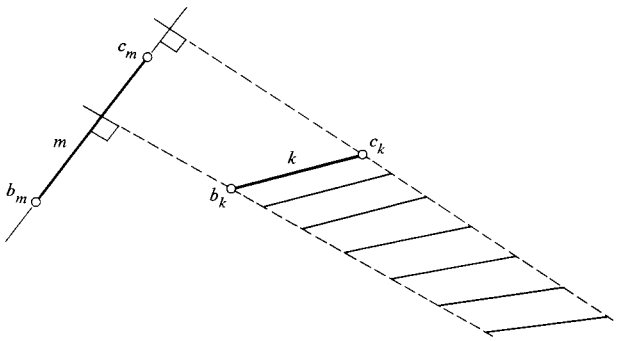

Figure 3 Area associated with two conductor segments.

Flux area of partial inductance

It is vital for an understanding of the concept of partial inductances to establish the relation to the flux area associated with partial inductances. The case of two straight, not necessarily coplanar, segments (shown in Fig. 3) is considered first.

• *Theorem:*

Given a thin straight conductor segment k between the points b_k and c_k, and given a second conductor segment between b_m and c_m, then

$$L_{\mathrm{p}_{km}} = \frac{1}{I_m} \int_{a_{k'}} \mathbf{B}_{km} \cdot d\mathbf{a}_{k'} ,$$

where $a_{k'}$ is the area bounded at the ends by the conductor segment k and infinity, and on the sides by two straight lines which go through the points b_k and c_k and the normal to the line connecting the points b_m and c_m as shown in Fig. 3. Then, alternatively:

$$L_{\mathrm{p}_{km}} = \frac{\mu}{4\pi} \int_{b_m}^{c_m} \int_{b_k}^{c_k} \frac{|d\mathbf{l}_k \cdot d\mathbf{l}_m|}{r_{km}} .$$

The proof is based on Stokes' theorem, which relates the surface integral over $a_{k'}$ to a line integral over l_k. The vector potential is given by

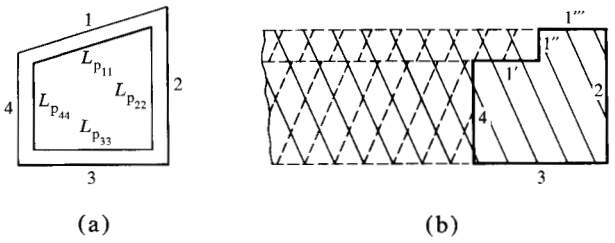

(a) (b)

Figure 4 (a) A closed loop with a tilted sigment. (b) Flux area associated with $L_{p_{11}}$, $L_{p_{22}}$, $L_{p_{44}}$ and $L_{p_{24}}$.

$$\mathbf{A}_{km} = I_m \frac{\mu}{4\pi} \int_{b_m}^{c_m} \frac{d\mathbf{l}_m}{r_{km}},$$

which is similar to Eq. (2), and therefore

$$\int_{a_{k'}} \mathbf{B}_{km} \cdot d\mathbf{a}_{k'} = I_m \frac{\mu}{4\pi} \oint_{l_k} \int_{b_m}^{c_m} \frac{d\mathbf{l}_m \cdot d\mathbf{l}_k}{r_{km}}.$$

It must then be shown that the path l_k can be restricted to the portion from b_k to c_k. $\mathbf{A}_{km}$ is zero at infinity, which implies that no contribution results from this portion of the loop. On the two paths perpendicular to the conductor m, $\mathbf{A}_{km}$ is in the direction of $\mathbf{l}_m$ and therefore normal to $d\mathbf{l}_k$, and thus the contribution to the integral is again zero. The integration over the loop l_k reduces, therefore, to integration over the path from b_k to c_k, as was to be shown.

The significance of the flux through the closed loop of Fig. 4(a) in relation to the flux associated with the partial inductances is brought out in the example below. Segment 1 in Fig. 4(a) is assumed to be tilted for generality. Equation (13) gives the total loop inductance in terms of partial inductances, which for this case is

$$L_{\text{loop}} = \sum_{k=1}^{4} \sum_{m=1}^{4} S_{km} L_{p_{km}}. \tag{14}$$

Each of the partial inductances has a flux area associated with it in accordance with the above theorem. Specifically, the areas associated with conductors 2 and 4 are considered. The tilted conductor segment 1 in Fig. 4(a) introduces an additional complication since this portion must be approximated by an infinite number of minute steps. In this example, only a finite single step is shown for clarity. The flux area associated with the partial self-inductance $L_{p_{22}}$ extends from somewhere near the conductor to infinity, since the partial self-inductance given by Eq. (12) is the average mutual inductance over the cross section of the conductor. The sign rule leads to a negative mutual inductance $L_{p_{24}}$ and the corresponding flux area extends from conductor 4 to infinity. Therefore, the flux areas cancel outside of conductor 4 and the only remaining flux area is restricted to the inside of the loop, as is expected. The same principle can be applied to conductor 1, where 1″ cancels the flux area outside instead of conductor 4. If this concept is applied to all partial inductances in Eq. (14), it is found that the only remaining flux area is restricted to the inside of the loop.

If nonplanar loops are considered, canceling pairs of currents can be introduced which reduce the general problem to a new set of locally planar loops. This is analogous to the usual proof of Stokes' theorem in terms of internal currents.

The last topic to be discussed in this section is incomplete loops. For example, the loops in Fig. 1 are all open at the connections. A difficult problem occurs if the length of the space between connection terminals is comparable to the dimensions of the loop, and this is actually quite common in integrated circuits. Often, the external connections are not specified, or are subject to variation among different applications. It is nevertheless desirable to characterize the inductance of such open loops.

Two definitions are introduced at this point. Fortunately, the concepts of partial inductance lead to a value for the inductance even if the loops are open.

• *Definition of open loop inductance*

Open loop inductance is defined as the inductance of an incomplete loop computed in accordance with the concepts of partial inductance.

It is apparent from the above development that the open loop inductance is the closed loop inductance with the partial inductances of the closing path removed. Thus, as an alternate solution, the inductance of an open loop can be calculated by defining a reasonable closing path. Then, however, the closing path must be completely specified. This approach leads to values of inductance appropriate to specific cases, but the open loop inductance appears to be an easier general way to specify inductance.

Another definition is helpful for the situation where the terminals are close together compared to the loop size.

• *Definition of inductance for a quasi-closed loop*

The inductance of a quasi-closed loop is obtained by simply ignoring the partial inductance between the terminals.

Unfortunately, if a loop is quasi-closed, it does not mean that the loop is decoupled from the connections to the loop. The only situation for which conductors are locally decoupled is that in which they are perpendicular to each other.

5. Evaluation of partial self-inductances

Partial self-inductances are evaluated from the definition of partial inductance, Eq. (12), where integration i and

integration j are both over the same conductor, or

$$L_{p_{ii}} = \frac{\mu}{4\pi}\frac{1}{T^2W^2}\int_{a_i}\int_{a_{i'}}\int_0^l\int_0^{l'}\frac{|d\mathbf{l}_i \cdot d\mathbf{l}_{i'}|}{r_{ii'}}\,da_i\,da_{i'}\,.$$

Partial self-inductance is the only case for which the integrand is singular due to integration over the same volume. The most important geometry of interest is a rectangular conductor, which is shown in Fig. 5. The solution of the six-fold integration is in general obtained by introducing new variables u_γ of the form $u_\gamma = \gamma - \gamma'$, where $\gamma = x, y, z$. Use was made here of a closed form answer given in [8]. From this, a new formulation is developed suitable for fast digital computations. Further, the accuracy of this formulation for long thin conductors is substantially improved. The following normalizations are introduced: $u \equiv l/W$ and $\omega \equiv T/W$. The partial inductance is then

$$\begin{aligned}\frac{L_{p_{ii}}}{l} = \frac{2\mu}{\pi}\Bigg\{&\frac{\omega^2}{24u}\left[\ln\left(\frac{1+A_2}{\omega}\right) - A_5\right] \\ &+ \frac{1}{24u\omega}\left[\ln(\omega + A_2) - A_6\right] + \frac{\omega^2}{60u}(A_4 - A_3) \\ &+ \frac{\omega^2}{24}\left[\ln\left(\frac{u+A_3}{\omega}\right) - A_7\right] + \frac{\omega^2}{60u}(\omega - A_2) \\ &+ \frac{1}{20u}(A_2 - A_4) + \frac{u}{4}A_5 - \frac{u^2}{6\omega}\tan^{-1}\left(\frac{\omega}{uA_4}\right) \\ &+ \frac{u}{4\omega}A_6 - \frac{\omega}{6}\tan^{-1}\left(\frac{u}{\omega A_4}\right) + \frac{A_7}{4} - \frac{1}{6\omega}\tan^{-1}\left(\frac{u\omega}{A_4}\right) \\ &+ \frac{1}{24\omega^2}\left[\ln(u + A_1) - A_7\right] + \frac{u}{20\omega^2}(A_1 - A_4) \\ &+ \frac{1}{60\omega^2 u}(1 - A_2) + \frac{1}{60u\omega^2}(A_4 - A_1) \\ &+ \frac{u}{20}(A_3 - A_4) \\ &+ \frac{u^3}{24\omega^2}\left[\ln\left(\frac{1+A_1}{u}\right) - A_5\right] \\ &+ \frac{u^3}{24\omega}\left[\ln\left(\frac{\omega + A_3}{u}\right) - A_6\right] \\ &+ \frac{u^3}{60\omega^2}\left[(A_4 - A_1) + (u - A_3)\right]\Bigg\}, \end{aligned} \tag{15}$$

where

$$A_1 \equiv (1 + u^2)^{\frac{1}{2}};$$

$$A_2 \equiv (1 + \omega^2)^{\frac{1}{2}};$$

$$A_3 \equiv (\omega^2 + u^2)^{\frac{1}{2}};$$

$$A_4 \equiv (1 + \omega^2 + u^2)^{\frac{1}{2}};$$

$$A_5 \equiv \ln\left(\frac{1+A_4}{A_3}\right);$$

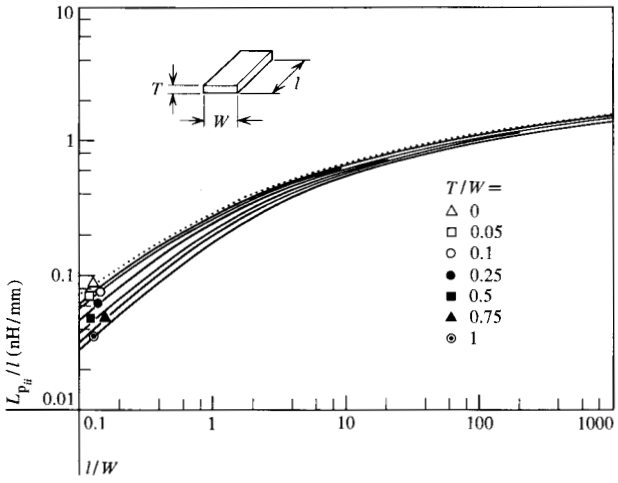

Figure 5 Partial self-inductance $L_{p_{ii}}$ for rectangular conductors.

$$A_6 \equiv \ln\left(\frac{\omega + A_4}{A_1}\right); \text{ and}$$

$$A_7 \equiv \ln\left(\frac{u + A_4}{A_2}\right).$$

The evaluation of Eq. (15) should be performed by summing from beginning to end, where the new terms are added to the sum of the previous terms. The results, shown in Fig. 5, were obtained on an IBM System/360 computer in double precision. Since the errors become large for very large values of u and for small values of ω, a second formulation is given for infinitely thin conductors that is applicable with a small error for $\omega \leq 0.01$. The formulation, based on the assumption that $\omega = 0$, e.g. [8], is

$$\begin{aligned}\frac{L_{p_{ii}}}{l} = \frac{\mu}{6\pi}\Bigg\{&3\ln\left[u + (u^2+1)^{\frac{1}{2}}\right] + u^2 + u^{-1} \\ &+ 3u\ln\left[\frac{1}{u} + \left(\frac{1}{u^2} + 1\right)^{\frac{1}{2}}\right] - \left[u^{\frac{4}{3}} + \left(\frac{1}{u}\right)^{\frac{2}{3}}\right]^{\frac{3}{2}}\Bigg\}. \end{aligned} \tag{16}$$

The normalizations are the same as in Eq. (15). The dotted line in Fig. 5 shows the evaluation of Eq. (16). Simplified formulas are available for many other situations. For example, the inductance of a round wire of length l and diameter W given by $L_{p_{ii}}/l = (\mu/2\pi)\,[\ln(4u) - 1]$ approximates Eq. (15) for $u > 10$ and $\omega = 1$.

Next, a formulation for partial self-inductance for conductors of an arbitrary cross section is developed to extend the usefulness of the theory. Use is made of the above result for rectangular conductors.

• *Theorem for conductors of arbitrary cross section*
Given a straight conductor k of length l with an arbitrary cross section, let the conductor cross section be approxi-

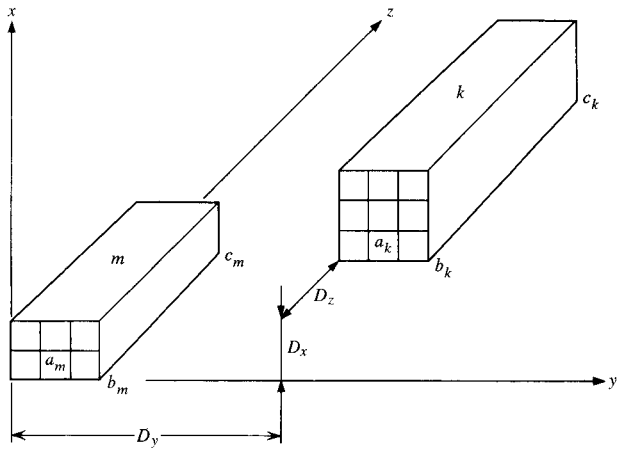

Figure 6 Partitioning of areas a_m and a_k.

mated by a set of subconductors each having rectangular cross section; then the partial self-inductance is given by

$$L_{p_{kk}} = \left[2 \sum_{i=1}^{N-1} \sum_{j=i+1}^{N} \text{cof } L_{p_{ij}} + \sum_{i=1}^{N} \text{cof } L_{p_{ii}}\right]^{-1} \det L_p , \quad (17)$$

where cof indicates the cofactor of the element in the matrix and det is the determinant.

The proof is based on the definition of inductance

$$L_{p_{kk}} = V \Big/ s \sum_{i=1}^{N} I_i$$

since the voltage drop along the subconductors is related to the current vector by $\mathbf{V} = s\mathbf{L}_p\mathbf{I}$ and since all voltages along the conductors are equal to $V_i = V$. Use is made also of the symmetry of the matrix of "partial subinductances." This symmetry is evident from Eq. (12).

Thus, self-inductances for arbitrary conductor cross sections can be calculated with the aid of Eqs. (15) and (17).

6. Computation of partial mutual inductances

A multitude of geometries must be considered for the computation of partial mutual inductances because of the many possible relative conductor locations. A useful collection of closed form answers for rectangular conductors is given in [8]. However, closed form solutions for mutual inductances become even more extensive than Eq. (15) with a corresponding increase in errors. Below, a new filament approximation is developed which is convenient for computer implementation. (Filament approximations used in the past were mostly developed to facilitate hand calculations.) Further, a scheme is developed by which the accuracy of the solution can be found. The line integrals inside the area integrations in Eq. (12) are defined as

$$L_{pf_{ij}} \equiv \frac{\mu}{4\pi} \int_{b_i}^{c_i} \int_{b_j}^{c_j} \frac{|d\mathbf{l}_i \cdot d\mathbf{l}_j|}{r_{ij}} , \quad (18)$$

in accordance with Eq. (5). $L_{pf_{ij}}$ can be viewed as the inductance between any two filaments of the two different conductors for which the mutual inductance is to be calculated.

The conductor cross sections a_k and a_m are partitioned into a set of rectangles as shown in Fig. 6, and a simple formulation is obtained when Eq. (12) is rewritten as a sum,

$$L_{p_{km}} = \lim_{\substack{K\to\infty \\ M\to\infty}} \frac{1}{KM} \sum_{i=1}^{K} \sum_{j=1}^{M} L_{pf_{ij}} , \quad (19)$$

where K and M correspond to conductors k and m respectively.

For a practical evaluation of Eq. (19) only a finite number of filaments is used. In fact, accurate calculations can be obtained with a small number of filaments, as is shown below. Also, a reciprocal relation exists between accuracy and computation time. A closed form solution for the filament inductance, e.g. [1], is

$$\frac{L_{pf_{mk}}}{l_m} = \frac{\mu}{4\pi} \sum_{i=1}^{4} \{(-1)^{i+1} g_i \log [g_i + (g_i^2 + r^2)^{\frac{1}{2}}] - (g_i^2 + r^2)^{\frac{1}{2}}\} , \quad (20)$$

where

$g_1 = 1 + p$;

$g_2 = 1 + p - v$;

$g_3 = p - v$; and

$g_4 = p$.

The normalizations used are $v \equiv \frac{l_k}{l_m}$, $p \equiv \frac{Dz}{l_m}$ and

$r \equiv [(x_m - x_k)^2 + (y_m - y_k)^2]^{\frac{1}{2}} / l_m$,

where $(x_m - x_k)$, $(y_m - y_k)$ and Dz designate the respective differences in the filament coordinates and l_m and l_k are the lengths of the filaments. The accuracy of the evaluation of Eq. (19) for fixed K and M depends on the relative position of the conductors. Examples for the two cases requiring the largest number of filaments are shown in Figs. 7 and 8. This suggests that the number of filaments per conductor is chosen to be an inverse function of the distance between conductors. This results in a considerable reduction in the necessary number of computations, since only a small number of conductors can be physically close together in a multiconductor situation. Very few filaments are needed for accurate calculations at distances between the conductors that are larger than the cross sectional dimensions. In this case, partial mutual inductance is a weak function of the

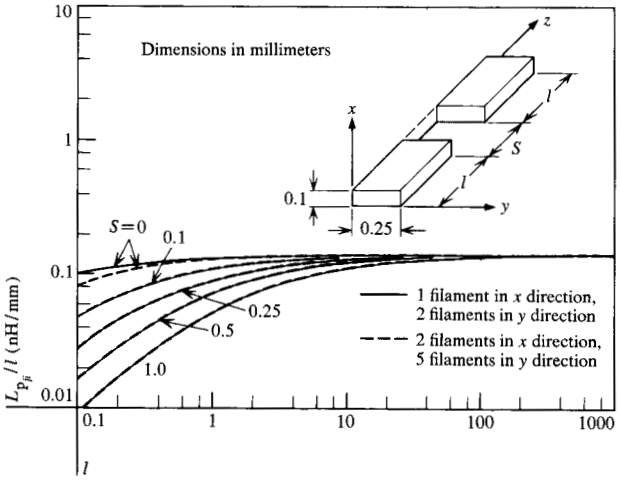

Figure 7 Comparison of approximations for mutual inductances.

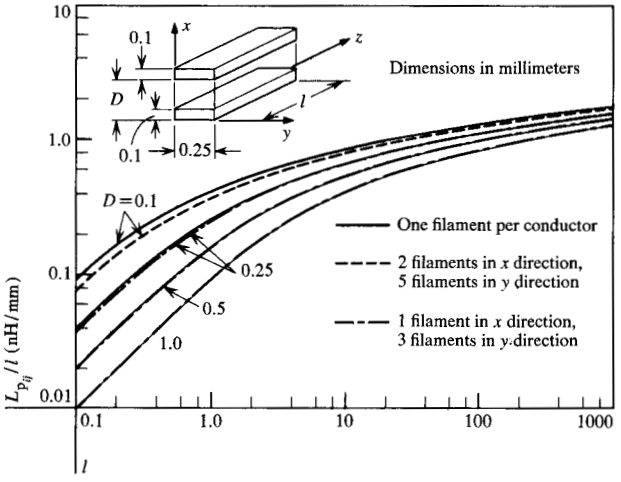

Figure 8 Comparison of approximations for mutual inductances.

conductor cross sections. A heuristic algorithm is easily developed for the selection of an appropriate number of filaments for each geometry.

Further, the formulation given above suggests immediately an extension of the concepts to conductors of any cross section. The partial mutual inductance can be found by representing a conductor in terms of a set of filaments in the direction of current flow. This assumes, however, that the direction of current flow is known. It is thus noted that this formulation includes arbitrary cross sections for all conductors, at least in an approximate sense.

The remainder of this section is devoted to evaluating the accuracy of the filament solution. In essence, the formulations given below are used to compare the accuracy of the filament representation, Eq. (19), with closed form answers for the worst case positions shown in Figs. 7 and 8.

To start with, a formulation for conductors on a common axis is developed, as is shown in Fig. 7. Then the computation of the mutual inductances is related to the self-inductances as follows:

• *Theorem for conductors on the same axis*

Given two conductors k and m on the same axis of lengths l_k and l_m, with cross sections identical but arbitrary ($a_k = a_m \equiv a$), let the partial self-inductance of a conductor i with cross section a and length $l_i = l_k + l_m$ be called $L_{p_{ii}}$. Then, a)

$$L_{p_{km}} = \tfrac{1}{2}[L_{p_{ii}} - L_{p_{kk}} - L_{p_{mm}}],$$

if the two conductors are a continuation of each other, and b)

$$L_{p_{km}} = \tfrac{1}{2}[L_{p_{ll}} - L_{p_{qq}} - L_{p_{oo}} + L_{p_{nn}}],$$

Figure 9 Equivalent circuit for two conductors on same axis.

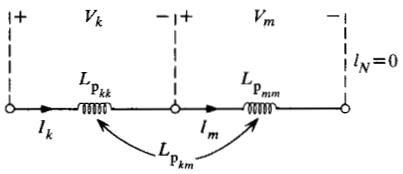

if the conductors are separated by a distance l_n. $L_{p_{ll}}$ is the inductance of a conductor of length $l_m + l_k + l_n$, and $L_{p_{oo}}$, $L_{p_{qq}}$ refer to conductors of length $l_m + l_n$ and $l_k + l_n$ respectively.

A proof is outlined for the simpler part a) of the theorem. The equivalent circuit for this case is shown in Fig. 9. The inductance of a conductor of length $l_n + l_m$ is then

$$L_{p_{ii}} = \left.\frac{V_k + V_m}{sI}\right|_{I=I_k=I_m} = L_{p_{mm}} + L_{p_{km}} + L_{p_{mk}} + L_{p_{kk}}.$$

The desired result follows immediately since $L_{p_{km}} = L_{p_{mk}}$.

Again, the curves in Fig. 7 can be obtained from this theorem and Eq. (15). The curves evaluated from the theorem coincide with the answers for two filaments in the x direction and five filaments in the y direction.

The other case of interest is the computation of the partial inductances between conductors with the relative locations shown in Fig. 8.

• *Theorem for parallel conductors*

Given two rectangular conductors with cross sections a_k and a_m of length l and with one parallel side touching, and $L_{p_{ii}}$ the self-inductance of a conductor of cross section $a_k + a_m$, then,

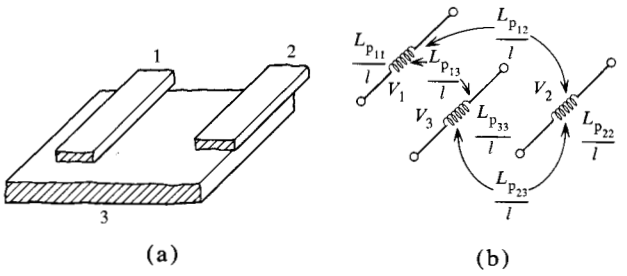

(a) (b)

Figure 10 (a) A two-dimensional three conductor structure. (b) Equivalent circuit in terms of partial inductances.

$$L_{p_{km}} = L_{p_{ii}} + [L_{p_{ii}}^{\,2} + L_{p_{kk}} L_{p_{mm}} - L_{p_{ii}}(L_{p_{kk}} + L_{p_{mm}})]^{\frac{1}{2}}.$$

The proof is similar to the proof for the partial self-inductance theorem for arbitrary cross sections given above.

Again, the two theorems above are useful in determining the appropriate number of filaments for the representation of partial mutual inductances. Numerical calculations show that the filament representation works efficiently for all relative conductor locations, except the worst case position shown in Fig. 8 where both conductors are very thin. For the latter case, however, the conductors can be approximated to be infinitely thin and the inductance determined by a different formula. A closed form solution [8] leads to accurate partial inductances for this special case, which is mostly of interest in the two-dimensional formulation given in the next section.

7. Inductances of two-dimensional structures

The representation of any physical structure by an infinitely long two-dimensional model is clearly an approximation. This is especially true if a large number of parallel conductors are involved, since not all of them can be physically close (compared with their length) to all other conductors. The approximation of a set of conductors by a two-dimensional model can be very convenient, however, since the inductance matrix must be specified for a unit length only.

The formulation given below is not a true two-dimensional representation. The length will be set equal to the physical length of the actual geometry. This has the advantage that the sensitivity with respect to length of the inductance per unit length can be investigated. It is also noted that the conductors are assumed to be "quasi-closed" at both ends in the sense of the definition given above.

A section of a three-conductor geometry is shown in Fig. 10(a). The partial inductances in the equivalent circuit of Fig. 10(b) can be evaluated by the formulation given above. The matrix of partial inductances must be related to the inductance matrix **L**, which is usually specified for a set of coupled two-dimensional transmission lines having a common ground conductor. Conductor 3 in this example is assumed to be the common ground return path. The inductance matrix is then calculated from the system of partial inductances divided by the length l,

$$\mathbf{V} = s\mathbf{L}_p\mathbf{I} \tag{21}$$

and the sign rule as

$$\mathbf{L} = \begin{bmatrix} (L_{p_{11}} - L_{p_{13}} - L_{p_{31}} + L_{p_{33}}) & (L_{p_{12}} - L_{p_{13}} - L_{p_{32}} + L_{p_{33}}) \\ (L_{p_{21}} - L_{p_{23}} - L_{p_{31}} + L_{p_{33}}) & (L_{p_{22}} - L_{p_{23}} - L_{p_{32}} + L_{p_{33}}) \end{bmatrix} \tag{22}$$

The inductance matrix **L** for the general system with a common ground return is found by a generalization of the above example. The general system consists of N conductors with an inductance matrix of the order N-1. The common return conductor is chosen to be conductor k. Then, the elements of the inductance matrix are

$$L_{ij} = L_{p_{ij}} - L_{p_{ik}} - L_{p_{kj}} + L_{p_{kk}}, \tag{23}$$

where

$i, j = 1, 2, \cdots, N;$

$i, j \neq k.$

Very large ground conductors may present a problem in some cases. Judgment must be used in selecting an effective ground width in such a situation. The low-frequency inductances found here are an upper bound on the inductance as a function of frequency. The inductance matrix is usually calculated from the capacitance matrix [9,10]. This leads to the inductances at an infinite frequency, which is a lower bound on **L**. Hence, the variation of inductance with frequency can be bounded from below and above. An example is given for six conductors located in parallel on a planar surface. All conductors are assumed to be 12.7μm thick and 50.8μm wide. The center-to-center spacing is chosen to be 152.4μm. Then, the inductance matrix corresponding to Eq. (23) is

$$\begin{bmatrix} 15.9 & & & & \\ 10.7 & 15.0 & & & \\ 8.74 & 9.69 & 13.9 & & \\ 7.09 & 7.48 & 8.31 & 12.2 & \\ 5.12 & 5.28 & 5.51 & 6.1 & 9.45 \end{bmatrix}$$

for an overall length of 3.81cm. The elements of the matrix are in nH/cm. If the same geometry is used, the

inductance matrix obtained from the capacitance matrix [10] is

$$\begin{bmatrix} 14.7 & & & & \\ 10.1 & 13.8 & & & \\ 8.15 & 9.06 & 12.7 & & \\ 6.54 & 6.89 & 7.68 & 11.1 & \\ 4.65 & 4.76 & 5.0 & 5.51 & 8.35 \end{bmatrix}$$

For this structure, the two bounds differ by less than ten percent. Also, a greater difference is noted in L_{66} for the conductor near reference conductor 6, compared to the conductors further away.

As a more general case, inductances can be evaluated between loops formed by the connection of sets of any two conductors at the far end. If we assume that one loop consists of conductors i and j and that a second loop is constructed with conductors k and l, then the loop inductances are

$$L_{ik} = L_{p_{ik}} - L_{p_{il}} - L_{p_{jk}} + L_{p_{il}}, \tag{24}$$

where $i, j, k, l = 1, 2, \cdots, N$, and I_i, I_k are in the same direction.

Errors may be introduced in Eqs. (23) and (24) if the resultant calculated mutual inductances are much smaller than the partial inductances on the right-hand side of the equation.

8. Inductance of three-dimensional geometries

All physical systems are three-dimensional in a strict sense. Besides the class of geometries considered in the last section (which can be represented by two-dimensional approximations), there exists a large class of problems which must be solved in three dimensions. Figure 11 shows two conductors which are considered to be of a general N-loop system. This example illustrates some of the difficulties common to many physical structures that must be characterized. Loop 1 in Fig. 11 forms a quasi-closed loop according to the definition, since the gap is small. Loop 2 is an open loop and, therefore, the open loop inductance can be evaluated for this case. It seems appropriate to close the path as indicated in Fig. 11(a), since a more realistic value of inductance is obtained. The cross section of the closing path must also be specified to completely characterize the situation. It should be noted, however, that this path is only specified in lieu of further information concerning the continuation of the conductors. Conceivably, the entity shown in Fig. 11 may be wired into different configurations.

All inductances of the system can be evaluated from

$$L_{ij} = \sum_{k=1}^{K} \sum_{m=1}^{M} S_{km} L_{p_{km}} \tag{25}$$

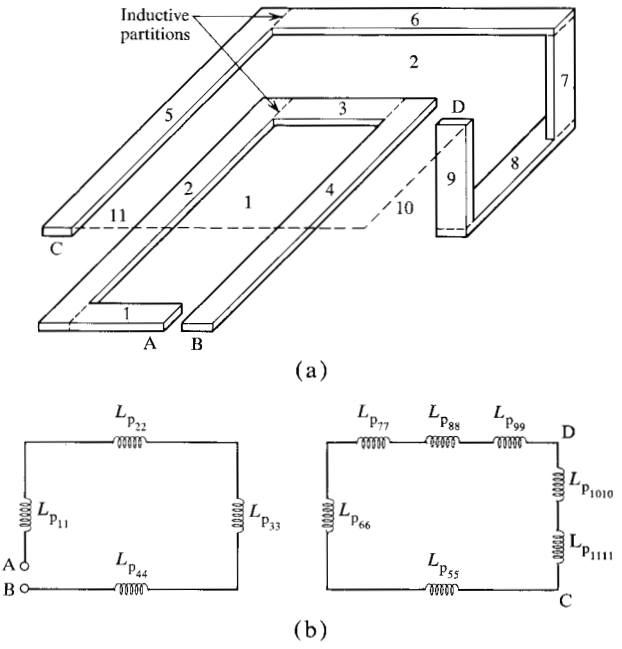

Figure 11 (a) Two loops of a system and (b) equivalent circuit.

for the partitions shown in Fig. 11. Again, loop i has K partial conductors while loop j consists of M partial conductors. This analysis is, at least in an approximate sense, applicable to any interconnection system. A simple example is given in Fig. 12. Since only a few configurations of interest can be discussed here, it is generally noted that the partial inductances themselves follow the rules of network analysis. Thus, algorithms for other configurations can easily be developed.

9. Measurement of small inductances

Most conventional inductance bridges fail to give accurate readings for inductances of a value less than about 100 nH. Errors are mainly the result of coupling between the instrument and the unknown inductance.

Measurements are possible, however, with a conventional bridge if the unknown loop is planar and is placed at such a distance from the instrument (as shown in Fig. 13) that coupling is negligible. A coupling loop is placed perpendicular to both the unknown and the instrument, in such a way that the perpendicular conductor segments are decoupled. Two measurements are required. For the first measurement, the terminals are shorted with conductor 4 (shown dashed in Fig. 13). With the assumption that the instrument can be represented by a single partial inductance $L_{p_{11}}$, the shorted loop inductance is

$$L_{sh} = \sum_{i=1}^{4} L_{p_{ii}} - 2\, L_{p_{23}} \tag{26}$$

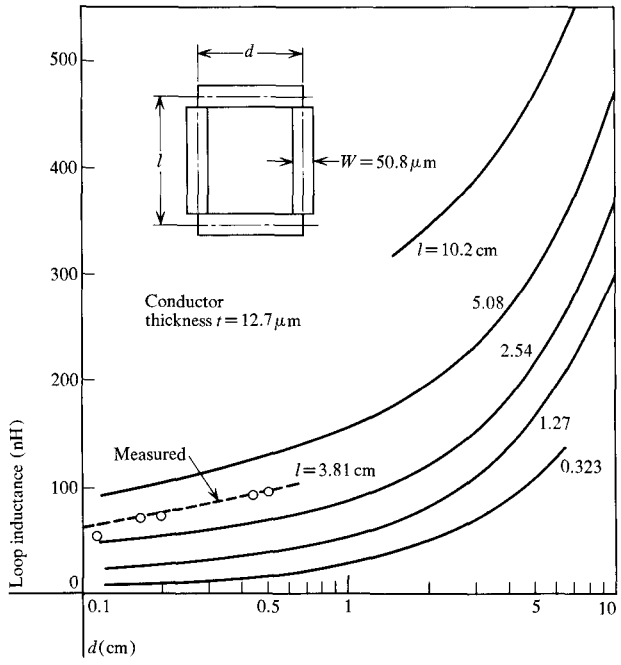

Figure 12 Inductance of a rectangular loop.

Figure 13 Measurement of small inductances.

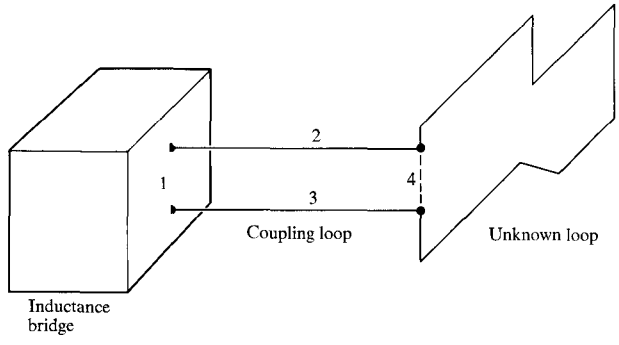

if $L_{p_{14}}$ is small due to the large distance.

A second measurement with the unknown loop of an inductance L_{loop} connected, and $L_{p_{44}}$ removed, leads to the total inductance

$$L_{Total} = L_{sh} - L_{p_{44}} + L_{loop} \tag{27}$$

if the coupling between $L_{p_{11}}$ and the unknown is small. Then, the inductance of the unknown is easily found as

$$L_{loop} = L_{Total} - L_{sh} + L_{p_{44}}. \tag{28}$$

It is noted that L_{sh} and $L_{p_{44}}$ are independent of the unknown, and therefore an a priori calibration is possible. Also, the measured inductance L_{loop} will be the open loop inductance according to the definition given above.

The measured values of inductances shown in Fig. 12 have been found by the technique described above.

10. Conclusions

Inductances in a microcircuit environment are of interest for many reasons. The major motivation for this work was to develop a means for determining inductive voltage drops and inductively coupled voltages for a large number of loops.

As stated in the introduction, a theory of inductance calculations for small inductance values has been developed. This theory concerns itself with so-called partial inductances, which represent the basic building blocks into which a system of conductors can be artificially subdivided to permit inductance calculations for complex geometries. The theory of partial inductances as presented in this paper is directed toward the circuit designer or the engineer concerned with overall systems performance. Chief among its advantages is the fact that very complex geometries can now be easily dealt with. Further, the analysis has been designed for digital computation, which represents an advantage over previous work that dates prior to the time when digital computers were widely available. To cite a further example of the usefulness of partial inductances, the inductance of open loops on integrated circuits can be uniquely characterized.

To review, the geometries considered have been mathematically described, at least in an approximate sense, by a set of straight conductor segments with a locally constant cross section. Current has been assumed to flow in the direction of the axes of the conductors. Further, sharp corners have been approximated in the most convenient way, since the extent of the corners is mostly small compared to the length of the conductors. Conductors of an arbitrary cross section can be included by the formulation given here. Also, the method is not limited to simple arrangements since partial inductances follow the rules of network analysis. However, approximations are necessary in many cases.

All the necessary expressions for a computer implementation of the concepts have been given here.

Acknowledgments

The author wishes to thank M. Handelsman for reading the manuscript and for many helpful discussions on the subject. Acknowledgment is also given to J. Eidsheim, J. Tzeng, T. Ehling and A. Plaza for their kind cooperation during the course of this work.

References

1. F. Grover, *Inductance Calculations: Working Formulas and Tables*, Dover, New York 1962.
2. E. Weber, *Electromagnetic Theory*, Dover, New York, 1965.

3. A. E. Ruehli, *IEEE Intl. Solid State Circuits Conf. Digest*, Lewis Winner, New York 1972, p. 64.
4. M. Caulton, B. Hershenov, S. P. Knight, R. E. DeBrecht, *IEEE Trans. Microwave Theory Tech.* **MTT-19,** 588 (1971).
5. W. A. Perkins, J. C. Brown, *J. Appl. Phys.* **35,** 3337 (1964).
6. S. Ramo, J. Whinnery and T. van Duzer, *Fields and Waves in Communication Electronics*, McGraw-Hill Publishing Co., Inc., New York 1965.
7. N. Balabanian and T. Bickart, *Electrical Network Theory*; John Wiley and Sons, Inc., New York 1969.
8. C. Hoer and C. Love, *J. Res. Natl. Bureau Standards* **69C,** 127 (1965).
9. Y. M. Hill, N. O. Reckord and D. R. Winner, *IBM J. Res. Develop.* **13,** 314 (1969).
10. W. T. Weeks, *IEEE Trans. Microwave Theory Tech.* **MTT-18,** 35 (1970).

Received November 4, 1971

The author is located at the IBM Thomas J. Watson Research Center, Yorktown Heights, New York 10598.